Journal of Hepatology 2000; **33**: 254–265
Printed in Denmark · All rights reserved
Munksgaard · Copenhagen

Journal of Hepatology
ISSN 0168-8278

p53 but not p16^{INK4a} induces growth arrest in retinoblastoma-deficient hepatocellular carcinoma cells

Anne Pierre Morel[1*], Kezban Unsal[2*], Tolga Cagatay[2], Frederique Ponchel[1], Brian Carr[3] and Mehmet Ozturk[1,2]

[1]*INSERM U453, Centre Leon Berard, Lyon, France,* [2]*Department of Molecular Biology and Genetics, Bilkent University, Ankara, Turkey, and* [3]*Pittsburgh Transplantation Institute, University of Pittsburgh, Pittsburgh, PA, USA*

Background/Aim: **Both p16^{INK4a} and p53 proteins are negative regulators of the cell cycle. In human hepatocellular carcinomas (HCC), the loss of function of p53, retinoblastoma (pRb) and p16^{INK4a} genes by different mechanisms has been largely documented, but their hepatocellular effects are poorly known. We compared the growth-inhibitory effects of p16^{INK4a} and p53 proteins in Hep3B cell line-derived clones.**
Methods: **Cells were transfected with inducible p16^{INK4a} and p53 expression vectors, and stable clones were analyzed for transgene expression by Western blotting and immunoperoxidase staining. Effects on cell growth were analyzed by *in vitro* growth assay, thymidine incorporation and flow cytometry. Biochemical effects of p53 were tested by Northern blotting of p21^{Cip1} transcripts and by Western blotting of p21^{Cip1}, mdm-2, bax, cyclin-dependent kinase 2 and cyclin E proteins. The pRb protein was studied by Western blotting and immunoprecipitation assays.**
Results: **The induction of p16^{INK4a} protein expression did not affect *in vitro* growth of cells. In contrast, p53 protein in its wild-type conformation provoked a growth arrest accompanied by transactivation of p21^{Cip1} gene and accumulation of p21^{Cip1}, bax and mdm-2 proteins. p53-induced growth arrest was due to a cell cycle arrest at the G1/S transition, probably mediated by p21^{Cip1} protein, which inhibits cyclin-dependent kinase 2/cyclin E complexes.**
Conclusions: **The lack of detectable pRb protein and resistance of cells to p16^{INK4a} strongly suggest that p53 is able to arrest the growth of HCC cells by a mechanism independent of "p53-retinoblastoma pathway". These findings are applicable to HCC with aberrations of both p53 and pRb genes, and may not represent the universal effects of p53 in hepatic cells.**

Key words: **Cell cycle arrest; Cyclin E; Hepatoma; p16^{INK4a}; p21^{Cip1}; p53; Retinoblastoma.**

HEPATOCELLULAR carcinoma (HCC), which is etiologically associated to hepatitis B virus (HBV), hepatitis C virus (HCV) and aflatoxins, is one of the most frequent cancers world-wide (1). Genetic studies have revealed so far that a dozen genes are altered in these cancers. These genetic alterations (mostly somatic) are related to at least four different pathways, including DNA damage response (p53 gene), cell cycle regulation (retinoblastoma, p16^{INK4a} and cyclin D genes), TGF-β (M6P/IGF2R, SMAD2 and SMAD4 genes) and wnt (β-catenin and APC genes) signaling pathways (2).

p53 was the first tumor suppressor gene found to be mutated in HCC (3). Many reports now indicate that the p53 gene, which is located at chromosome 17p, is somatically mutated in about 30% of HCCs worldwide (2). Both the frequency and the type of p53 mutations are different depending on the geographical location and suspected etiology of these tumors. An HCC-specific codon 249 mutation (AGG→AGT leading to p53–249Ser), suspected to be induced by aflatoxins, was found in most HCCs from geographical areas with a high incidence of HCC and a high risk of exposure to aflatoxins (4,5). The frequency of all p53 mutations in HCC varies between 15% in Europe and 42% in China (2). On the other hand, physical and functional interaction between p53 protein and HBx viral antigen has

* A. P. M. and K. U. contributed equally to this work.

Received 4 October; revised 17 December; accepted 24 December 1999

Correspondence: Mehmet Ozturk, Department of Molecular Biology and Genetics, Bilkent University, 06533 Bilkent Ankara, Turkey. Tel: 90 312 266 50 81.
Fax: 90 312 266 50 97. e-mail: ozturk@fen.bilkent.edu.tr

been reported. Based on this experimental evidence, viral inactivation of wild-type p53 in HCC has been proposed (6–8).

The p53 protein is a transcription factor that enhances the rate of transcription of different genes that carry out, at least in part, the p53-dependent functions in a cell. Most of the p53 mutations in HCC, as in other cancers, occur in the central DNA binding domain, leading to a loss of its transcriptional activity. The p53 protein functions to integrate cellular responses to stress, such as exposure to DNA damaging agents and hypoxia (9). Under normal conditions, p53 is rapidly degraded in cells by a mechanism that involves $p14^{ARF}$ and mdm-2 proteins. Upon cellular stress, p53 is modified post-transcriptionally, dissociates from mdm-2 protein, becomes more stable, migrates into the nucleus and transactivates its target genes (9,10). One of the outcomes of p53 activation is cell cycle arrest at G1 phase mediated by $p21^{Cip1}$ protein, which is an inhibitor of different cyclin-dependent kinases, including those involved in the phosphorylation of the retinoblastoma protein (pRb). The so-called "p53-retinoblastoma pathway" implicates an important role for pRb and its two related gene products, p107 and p130, in p53-mediated G1-S phase regulation (9). p53 also plays a role in triggering apoptosis under several different physiological conditions. The apoptotic role of p53 appears to be limited to certain cell types such as hematopoietic cells. There is also experimental evidence that p53-dependent apoptosis can occur as a response to the expression of a viral or cellular oncogene or the absence of a critical tumor suppressor gene product such as pRb (9). Studies on the response of HCC cells to p53 are limited in number, and observations from different laboratories are sometimes contradictory. For example, we reported that p53 acts as a growth suppressor in Hep3B cells (11) and p53-mediated apoptosis was reported in the same cell line in several reports (12–14). However, these observations were challenged by Friedman et al. (15), who reported that Hep3B cells were resistant to p53-mediated growth arrest and apoptosis.

The $p16^{INK4a}$ gene, which is located at chromosome 9p, codes for two alternatively spliced transcripts (see ref. 16 for a review). One of the transcripts is for $p16^{INK4a}$ protein, an inhibitor of cyclin-dependent kinase 4 (CDK4) and CDK6, whereas the other is $p14^{ARF}$ protein which regulates p53 stability (10,17). The $p16^{INK4a}$ status in HCC has been studied extensively. Both germ-line and somatic mutations of the $p16^{INK4a}$ gene were found in HCC patients. It was also reported that about 50% of HCC display *de novo* methylation of the $p16^{INK4a}$ gene, as observed in many other cancers (reviewed in ref. 2). As an inhibitor of CDK4 whose main substrate appears to be pRb protein, $p16^{INK4a}$ protein is an antagonist of cyclin D for CDK4 activation (17). Therefore, it is not surprising that retinoblastoma gene mutations and cyclin D gene amplifications also occur in HCC, albeit at lower frequencies (2). Thus, the main consequence of $p16^{INK4a}$ gene alterations is considered to be a loss of CDK4 inhibition. As a result, the phosphorylation of pRb by CDK4 is no longer regulated, leading to an increase in "free E2F" transcription factors involved in the progression of G1 phase of cell cycle and G1/S transition. The expression of $p16^{INK4a}$ progressively increases as cells undergo senescence (17). This suggests that the loss of $p16^{INK4a}$ function in HCC is related to cellular immortalisation. However, the effects of $p16^{INK4a}$ protein in hepatoma cells have not been reported yet. It is also unknown whether and how $p16^{INK4a}$ gene alterations affect the cellular functions of $p14^{ARF}$ protein (the product of alternatively spliced transcripts of the same gene), whose main role appears to be the activation of p53 protein.

In this report, we compare the effects of p53 and $p16^{INK4a}$ proteins of Hep3B and its derivative cell lines. Hep3B is a differentiated HCC cell line with integrated HBV DNA and deleted p53 gene (3). Its derivative Hep3B-TR is a TGF-β-resistant clone due to a homozygous deletions of TGF-β receptor type II (18). The status of the retinoblastoma gene in the Hep3B cell line is a matter of debate (15,19). Our main goal was to know whether $p16^{INK4a}$ and p53 proteins, known to be upstream regulators of "retinoblastoma growth control pathway", differ in their phenotypic effects in these cells. We demonstrate that p53, but not $p16^{INK4a}$ is able to suppress the growth of these HCC cells by cell cycle arrest at G1/S transition. We provide evidence that the resistance of cells to $p16^{INK4a}$ protein is correlated with the lack of pRb protein. The same observation also demonstrates that p53-induced growth arrest in Hep3B-TR cells occurs independently from the retinoblastoma growth control pathway.

Materials and Methods

Plasmid constructs

The plasmids pLTRp53cGval135 and pSV2neo (ref. 20) were a gift from M. Oren (Rehovot, Israel). The plasmid pAUCT/CCW was constructed by A. Fattaey (Charlestown, MA, USA). This plasmid contains a Tet Repressor-vp16 fusion cDNA under the control of CMV promoter. It also contains a multiple cloning site downstream to a promoter sequence composed of a Tet operator and CMV TATA box. The pAUCT/CCW also contains a Neo® gene allowing the selection of stable clones. A pBluescript plasmid containing human $p16^{INK4a}$ cDNA (a gift from A. Samarut, Lyon, France) was used for cloning of $p16^{INK4a}$ cDNA into pAUCT/CCW plasmid. The p16 cDNA insert was removed from the pBluescript plasmid by EcoRI-XhoI restriction enzyme digestion. Purified $p16^{INK4a}$ cDNA fragment was

then ligated with pAUCT/CCW plasmid, which was previously linearized by digestion EcoRI and XhoI restriction enzymes to obtain pAUCT-p16^{INK4a} plasmid. In the presence of tetracycline, the Tet repressor-Vp16 fusion peptide suppresses the expression of p16^{INK4a} protein. In the absence of tetracycline, the suppressive function is abolished.

Cell lines and antibodies

Hep3B, Hep3B-TR, Mahlavu, Huh-7 and Saos-2 cell lines were grown in MEM medium containing 10% fetal calf serum, 2 mM L-glutamine, 200 units/ml penicillin, and 200 μg/ml streptomycin under 5% CO_2, unless otherwise described. Antibodies to pRb (clone IF8 from Santa-Cruz, clones Ab-5 and Ab-6 from Calbiochem), p53 (clone Ab-1 from Calbiochem and HR 231; a gift from T. Soussi, Paris, France), p21^{Cip1} (Ab-1 to waf1 from Calbiochem), mdm-2 (2A10; a gift from B. Vasylyk, Strasbourg, France), bax (N-20 from Santa Cruz), p16^{INK4a} (Ab-1 from Calbiochem) and cyclin E (Ab-1 from Calbiochem) were used.

Generation of stable cell clones expressing p16^{INK4a} and p53 proteins

Appropriate plasmids (10–20 μg of total DNA) were transfected into cells by the calcium phosphate precipitation method. The plasmids pLTRp53cGval135 and pSV2neo were used at a ratio of 1:20. The plasmid pAUCT-p16^{INK4a} was used alone. The p53-transfected cells were selected at 39°C in the presence of G 418 (400 μg/ml). The p16^{INK4a} clones were selected in the presence of tetracycline (5 μg/ml) and G 418 (400 μg/ml).

Cell growth assays

For p16^{INK4a}, 3000 to 5000 cells were plated into 6-well plates. Starting with a low number of cells allowed to continue the experiment for at least 10 days without a cell death due to an overgrowth of these cells which are not contact inhibited at full confluence. Twenty-four hours after plating (time zero), the medium was changed and the cells were incubated in the absence or in the presence of tetracycline (5 μg/ml) for up to 10 days. The number of viable cells was determined by manual counting, using a hemocytometer, at time zero and at days 2, 4, 6, 8, and 10. As an alternative assay, the same cell lines were grown as described for 7 days, and cells were visualized *in situ* by methyl green staining after fixation in ethanol. For p53 experiments, cells were seeded in 60-ml Petri dishes (at three different cell densities ranging from 50 000 to 500 000 cells per dish) and grown overnight at 39°C. The following day (time zero), half of the plates were moved to a 32°C incubator and further incubated for 7 days. Colony forming cells were visualized as described by crystal violet staining.

In situ *thymidine incorporation assay*

Cells were plated and grown at the permissive temperature (39°C) for 24 h. The following day, half of the plates were kept at the same temperature and the cells in the other half were shifted to the non-permissive temperate (32°C). Cells were labeled with [^{3}H]-thymidine for 24 h before the arrest of the experiment at 24 h or 48 h, and studied *in situ* for thymidine incorporation. [^{3}H]-thymidine (2.5 μCi/ml; Amersham) was used to label 50 000 cells grown on cover slips overnight in 6-well plates. After 24 h labeling, cells were fixed in methanol: acetic acid (3:1), dried at room temperature and cover slips were transferred onto glass slides and exposed to a autoradiography emulsion (NTB2; Kodak) for several days and stained with Giemsa technique. Slides were then analyzed under a light microscope and used to obtain pictures.

Flow cytometry

Cytometric analyses following BrdU labeling was performed as described previously (21). Briefly, cells were labeled with BrdU (30 μM) for 1 h or 2 h, rinsed with PBS, detached from plates by trypsin incubation, rinsed with PBS and fixed in 70% (v/v) ethanol. Cells were rehydrated in PBS, incubated in 2 ml of 2N HCl, permeabilized in PBS containing 0.5% Tween-20 and 0.5% BSA and incubated with FITC-conjugated anti-BrdU antibody (from Becton-Dickinson). Then RNAse A (50 μg/ml) was added, followed by propidium iodide (25 μg/ml; from Sigma). Cells were analyzed using a flow cytometer (Facscalibur, Becton-Dickinson).

Northern blotting

Total RNAs were extracted by the guanidium isothiocyanate method. RNA samples (10 μg) were separated by electrophoresis through denaturing formaldehyde agarose gel and transferred to nylon membrane (Hybond-N; Amersham). Membranes were hybridized with [^{32}P]-labeled p21^{Cip1} cDNA, as described (21) and subjected to autoradiography.

Western blotting

Cell protein extracts were prepared in a lysis buffer containing 50 mM Tris-HCl, 0.25 M NaCl, 1 mM $CaCl_2$, 0.1% Triton X-100, 50 mM NaF and a cocktail of protease inhibitors, as described previously (22). Equal amounts (usually 100 μg) of proteins were then separated by SDS-polyacrylamide gel electrophoresis in a Tris-glycine buffer and transferred to PVDF membranes (Millipore) using a semi-dry transfer apparatus (Biorad), following the manufacturer's recommendations. Membranes were checked for equal amounts of protein transfer by staining with Ponceau-S, and blocked in TBS-T (0.05% Tween-20 in Tris-buffered saline) containing 5% non-fat dry milk for 2 h, then incubated with the appropriate antibody overnight at 4°C. The blots were then rinsed in TBS-T and incubated with a peroxidase-conjugated secondary antibody for 1 h at room temperature. After washing in TBS-T, detection was performed using the chemiluminescence method (ECL, Amersham), followed by exposure to X-ray film. For most experiments, the same PVDF membranes were used to test different proteins from the same SDS-PAGE gels.The HR231 monoclonal antibody which recognizes both human and mouse p53 was used for p53 detection (23).

Immunoprecipitation

Subconfluent cells were grown for 2 h in methionine-free medium containing 5% dialyzed fetal calf serum. Cells were labeled with 0.2 mCi/ml [^{35}S] methionine (Amersham) for 4 h in 10-cm culture dishes. Cells were then washed in PBS and proteins were extracted in 1 ml lysis buffer, prepared as described for Western blotting. Samples were precleared with 80 μl of 50% (v/v) protein-A-Sepharose suspension (Pharmacia) for 1 h at 4°C and 5 μl of anti-pRb mouse antibody was added to the supernatant. After overnight incubation on a rocker at 4°C and a 5-min centrifugation at 13 000 rpm, supernatants were added to Eppendorf tubes containing 80 μl of 50% (v/v) protein-A-Sepharose beads. Antigen-antibody complexes were captured by a 60 min of incubation at room temperature and the beads were pelleted by centrifugation. The beads were washed 4 times in lysis buffer and the immunoprecipitates were directly resuspended in Laemmli buffer, heated at 80°C for 5 min and loaded on SDS-polyacrylamide gels (7.5%). After electrophoresis, gel was processed with Amplify solution (Amersham), dried and subjected to autoradiography.

Results

Hep3B hepatoma cells are resistant to p16^{INK4a} overexpression

Randomly selected clones from pAUCT-p16^{INK4a} transfections into Hep3B cells were first analyzed for tetracycline-regulated expression of p16^{INK4a} protein by Western blotting. Saos-2 cell line extracts, which express p16^{INK4a}, but not pRb protein, were used as a positive control (24,25). As shown in Fig. 1A, five clones (clones 9, 20, 23, 33 and 34) displayed increased expression of p16^{INK4a} in the absence of tetracycline, as compared to the presence of 5 μg/ml tetracycline. Three clones (clones 9, 20 and 34) did not express de-

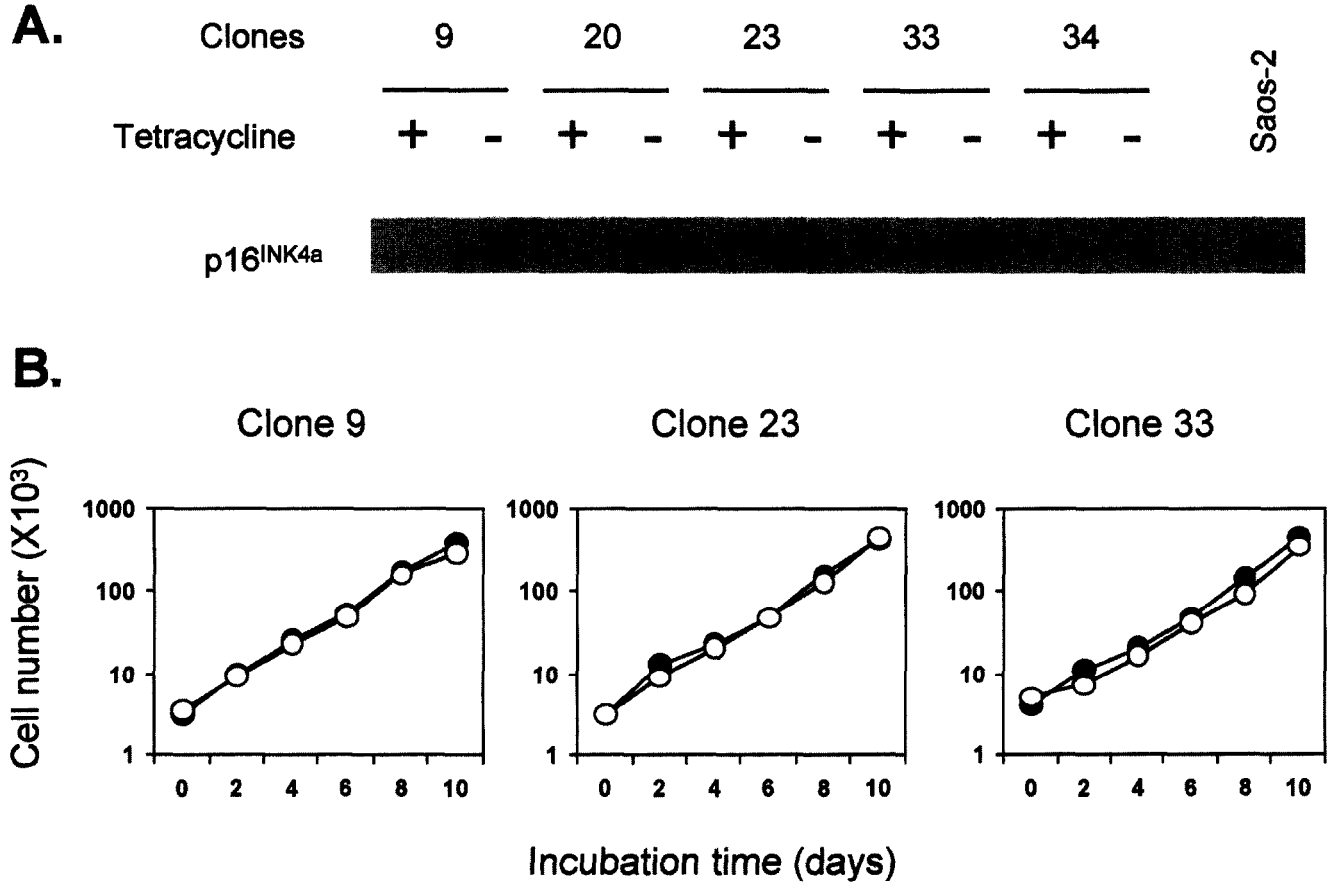

Fig. 1. Resistance of Hep3B-derived clones to p16-mediated growth inhibition. (A) Tetracycline-dependent expression of p16 in selected Hep3B clones. Cells were grown for 24 h in the absence (−) or in the presence (+) of 5 μg/ml tetracycline and cell lysates were tested for p16^{INK4a} protein by Western immunoblotting. Saos-2 cells were used as positive control. Equal protein loading was tested by Ponceau S staining. (B) The clones 9 (left), 23 (center) and 33 (right) were grown in the presence (filled circles) or the absence (open circles) of tetracycline for 10 days in 6-well culture dishes and the cell number was measured by manual counting at 2-day intervals.

tectable p16^{INK4a} protein in the presence of tetracycline, while clones 23 and 33 displayed weak immunoreactivity. In all clones tested, the levels of p16^{INK4a} were induced in the absence of tetracycline. The induction was strong in clones 20, 23 and 33, moderate in clone 9, but weak in clone 34. Clone 20 expressed p16^{INK4a} as a doublet.

Next, the effect of p16^{INK4a} overexpression on cell growth was tested using clones 9, 20, 23 and 33. For initial experiments, all four clones were grown in parallel in the presence or in the absence of tetracycline for 7 days and total number of cells were estimated by *in situ* staining. There was no apparent difference between the number of cells (data not shown), suggesting that p16^{INK4a} overexpression did not affect their growth rate. The lack of growth inhibition by p16^{INK4a} overexpression was confirmed by comparing growth rates of clones 9, 23 and 33 for 10 days and manual counting of cell numbers every 2 days. As shown in Fig. 1B, the growth rate of these clones was not affected by overexpression of p16^{INK4a} in the absence of tetracycline. These observations indicated that Hep3B cells are resistant to growth inhibitory effects of p16^{INK4a} protein.

Hep3B-TR cells are sensitive to p53-induced growth inhibition

To study the effects of wild-type p53, we used Hep3B-TR clone rather than the parental Hep3B cells, as Hep3B-TR clone is resistant to TGF-β (ref. 18). Apoptosis studies with Hep3B cells are complicated by the fact that these cells express TGF-β and may undergo apoptosis in the absence of wild-type p53 (22). To study p53 effects, we used as well-known and widely-used experimental model based on a mouse temperature-sensitive mutant p53-135val protein (20). Hep3B-

TR cells were transfected with the appropriate plasmids and eight G418-resistant clones were tested for p53 expression by Western blotting. As shown in Fig 2A, only three clones (TR1, TR3 and TR8) were positive initially. Our previous experiments indicated that certain cell lines tend to lose the expression of transfected plasmids during long-term culture (data now shown). Thus, it was important to test that the expression of p53 was stable and maintained during the *in vitro* growth of selected clones. TR1, TR3 and TR8 clones were grown for several weeks in the presence of G-418 and the expression of p53 was checked at different time points by immunoperoxidase staining with the anti-p53 monoclonal antibody HR 231 (ref. 23). As shown in Fig. 2B, the immunoperoxidase staining studies indicated that the expression of p53 was maintained at nearly 100% in TR3 cells, only 30% of TR8 cells maintained its expression, whereas TR1 cells lost p53 expression completely. Therefore, we performed the additional studies with TR3 and when needed with TR8 clone, in comparison to TR4 used as negative control (see Fig. 2A). To avoid any experimental error, TR3 and TR8 cells were checked regularly for the expression of p53 by immunoperoxidase staining throughout all the experiments described here.

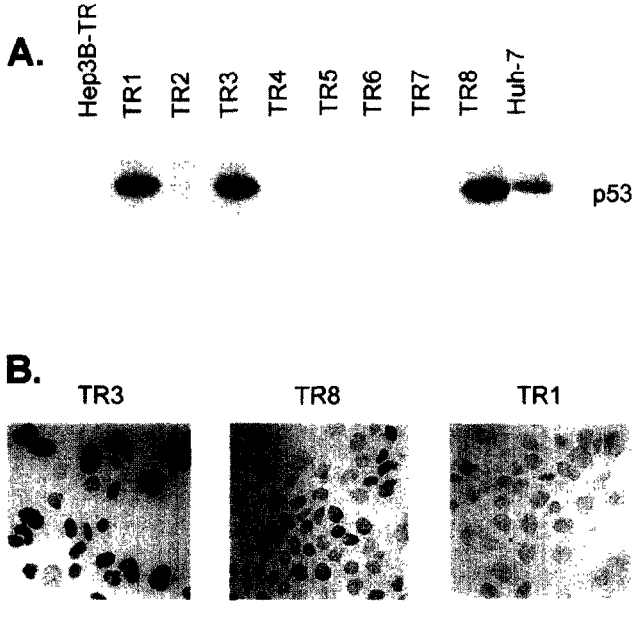

Fig. 2. Selection of Hep3B-TR clones stably expressing the mouse temperature-sensitive p53-135val protein (A) Neomycin-resistant clones were selected at the permissive temperature (39°C) and tested for p53 protein by Western blotting. Parental Hep3B-TR and Huh-7 cells were used as negative and positive controls, respectively. (B) p53-positive TR1, TR3 and TR8 clones were expanded in vitro *and cultured at the permissive temperature for several weeks, and the p53 expression was tested by indirect immunoperoxidase staining. The expression of p53 was fully retained in TR3 (left), but lost partially in TR8 (center), or totally in TR1 clone (right).*

First, we compared the growth of TR3 and TR4 clones by two different techniques after incubation of cells at either 32°C (non-permissive temperature, wild-type p53 conformation) or 39°C (permissive temperature, mutant p53 conformation). Initially, the effects of wild-type p53 on DNA synthesis were tested by thymidine incorporation studies. Radioactive [^{3}H]-thymidine was added to standard culture medium at times 0 and 24 h, following temperature-shift, and cells were grown for an additional 24 h in the presence of [^{3}H]-thymidine. Almost 100% of p53-negative TR4 cells were positive for thymidine incorporation at 24 h (Fig. 3a and b) as well as at 48 h (Fig. 3c and d), independent of temperature shift. TR3 cells grown at 39° also incorporated thymidine at a rate of about 100% at both 24 h (Fig. 3e) and 48 h (Fig. 3g). In contrast to these observations, the temperature shift to 32°C caused an almost total block of thymidine incorporation into DNA of TR3 cells, as early as 24 h (Fig. 3f). Only a few TR3 cells were positive at 48 h (Fig. 3h). These observations demonstrated that the activation of wild-type p53 in Hep3B-TR cells provoked a total loss of DNA synthesis.

To test the long-term effects of wild-type p53 expression, Hep3B-TR clones were grown at 32°C and 39°C for 7 days at different cell densities. When forced to grow at 32°C, the parental Hep3B-TR cells (Fig. 4a) as well as p53-negative TR4 clone (Fig. 4b) formed large colonies. In contrast, the p53-positive TR3 clone did not form colonies at 32°C, although single and scattered cells were still detectable after 7 days of culture (Fig. 4c). The growth inhibition of TR3 cells was due to the expression of wild-type p53 at 32°C in these cells which grew well and formed colonies at the permissive 39°C (Fig. 4d).

Taken together, these studies showed that p53 activation in TR3 cells induced a total loss of DNA synthesis and a permanent growth arrest. These cells did not display any visible evidence of p53-dependent apoptotic cell death during these experiments. Additional apoptosis experiments using morphological analysis, *in situ* DNA staining by H33258 and DNA ladder tests indicated that the apoptotic cell death was minimal (<5%) in all Hep3B-TR clones, independent of p53 status and growth temperature (data not shown). Next, we further explored the effects of wild-type p53 in Hep3B-TR clones through study of the expression of several known p53 target genes.

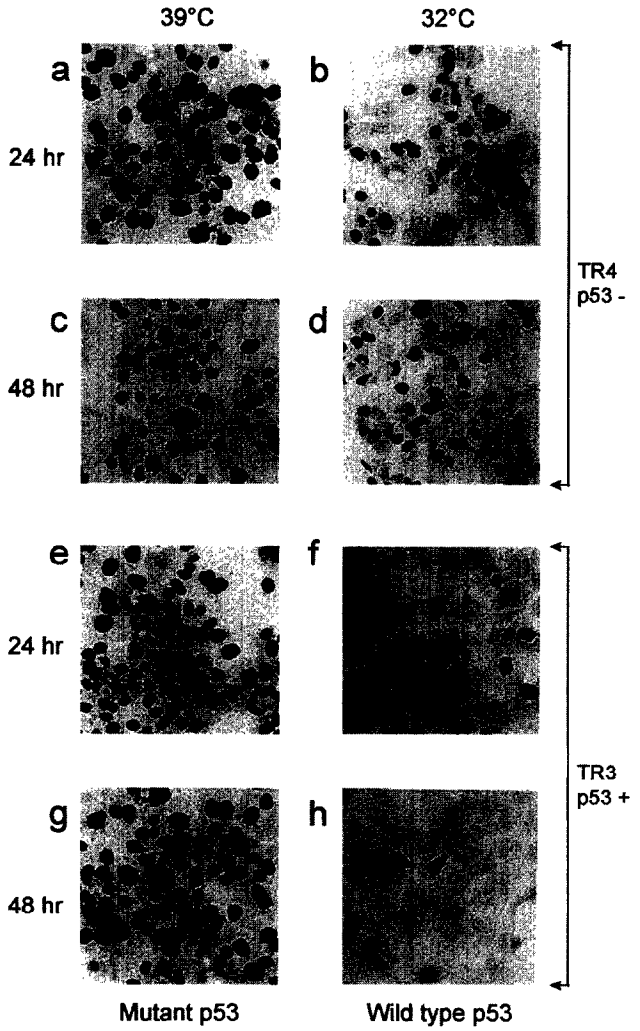

Fig. 3. p53 activation in TR3 cells at non-permissive temperature leads to an arrest of DNA synthesis. The p53-negative TR4 (a, b, c, d) and p53-positive TR3 (e, f, g, h) cells were plated and grown at the permissive temperature (39°C) for 24 h. The following day, half of the plates (a, c, e, g) were kept at the same temperature and the cells in the other half (b, d, f, h) were shifted to the non-permissive temperature (32°C). Cells were labeled with [^{3}H]-thymidine for 24 h before the arrest of the experiment at 24 h (a, b, e, f) or 48 h (c, d, g, h), and studied in situ *for thymidine incorporation. Note the loss of thymidine incorporation in TR3 cells at the non-permissive temperature (f, h), in contrast to TR4 cells (b, d).*

p53-dependent induction of mdm-2, $p21^{Cip1}$ and bax genes in Hep3B-TR clones

Among known p53 target genes, the expression of mdm-2, $p21^{Cip1}$ and bax were studied. Northern blot analysis of $p21^{Cip1}$ transcripts showed a strong induction of $p21^{Cip1}$ gene expression at 32°C in TR3 cells, but not in TR4 cells (Fig. 5). The $p21^{Cip1}$ transcripts were nearly detectable in both clones when grown at 39°C. Next, protein levels of mdm-2, $p21^{Cip1}$ and bax were tested under similar conditions. The mdm-2 protein was easily detectable in both parental Hep3B-TR and TR3 cells grown at 39°C (Fig. 6A). At 32°C, mdm-2 levels did not change significantly in Hep3B-TR and TR4 cells, although a slight increase at 48 h was seen with Hep3B-TR (Fig. 6A, data not shown for TR4). In contrast, there was a clear-cut increase of mdm-2 protein levels in TR3 cells when grown at the same non-permissive temperature at both 48 h and 72 h (Fig. 6A). A p53-dependent increase of mdm-2 levels was detectable as early as 24 h in these cells (data not shown).

Accumulation of protein products of two additional p53 target genes, namely $p21^{Cip1}$ and bax, was investigated following p53 activation in TR3 cells (Fig. 6B). At 39°C, $p21^{Cip1}$ protein was undetectable in both TR3 and TR4 cells. At 32°C, the expression of $p21^{Cip1}$ was strongly induced in TR3, but not in TR4 (Fig. 6B). In contrast to $p21^{Cip1}$, bax protein was present in both TR3 and TR4 clones grown at 39°C. At the non-permissive temperature (32°C), a weak increase in bax levels was observed in TR3, but not in TR4 cells (Fig. 6B).

Taken together, these studies demonstrated that the basal expression of $p21^{Cip1}$ gene in Hep3B-TR-derived clones was weak (low levels of transcripts, but no detectable $p21^{Cip1}$ protein). The activation of wild-type p53 provoked an immediate and strong accumulation of both $p21^{Cip1}$ mRNA and protein. In contrast, basal levels of bax protein in these cells were quite high and the activation of wild-type p53 resulted in a moderate increase. Thus, we reasoned that the growth arrest induced by p53 in TR3 cells was mainly due to the activation of $p21^{Cip1}$ gene.

p53-dependent cell cycle arrest in Hep3B-TR clones

To further analyze the growth response of TR3 cells to p53 activation, we studied their cell cycle profiles over a period of 3 days. Both TR3 and TR4 cells were first grown at 39°C for 24 h, and then half of the plates were kept at the same temperature and the other half transferred to 32°C. Cells were labeled at 24 h, 48 h and 72 h after temperature-shift. The BrdU-labeling was done for 1 h to 2 h at different time-points tested. Cell cycle distributions at different times were shown in Table 1. TR3 cells grown at 32°C displayed a drop in S phase cells from 29% to 4%, 23±5% to 9±4% and 20±6% to 11±5% at 24 h, 48 h and 72 h, respectively. Concomitantly, there was a moderate increase in both G1 and G2/M phase cells at all time points tested. This effect was dependent on p53 expression. Indeed, p53-negative TR4 cells showed an increase, rather than a

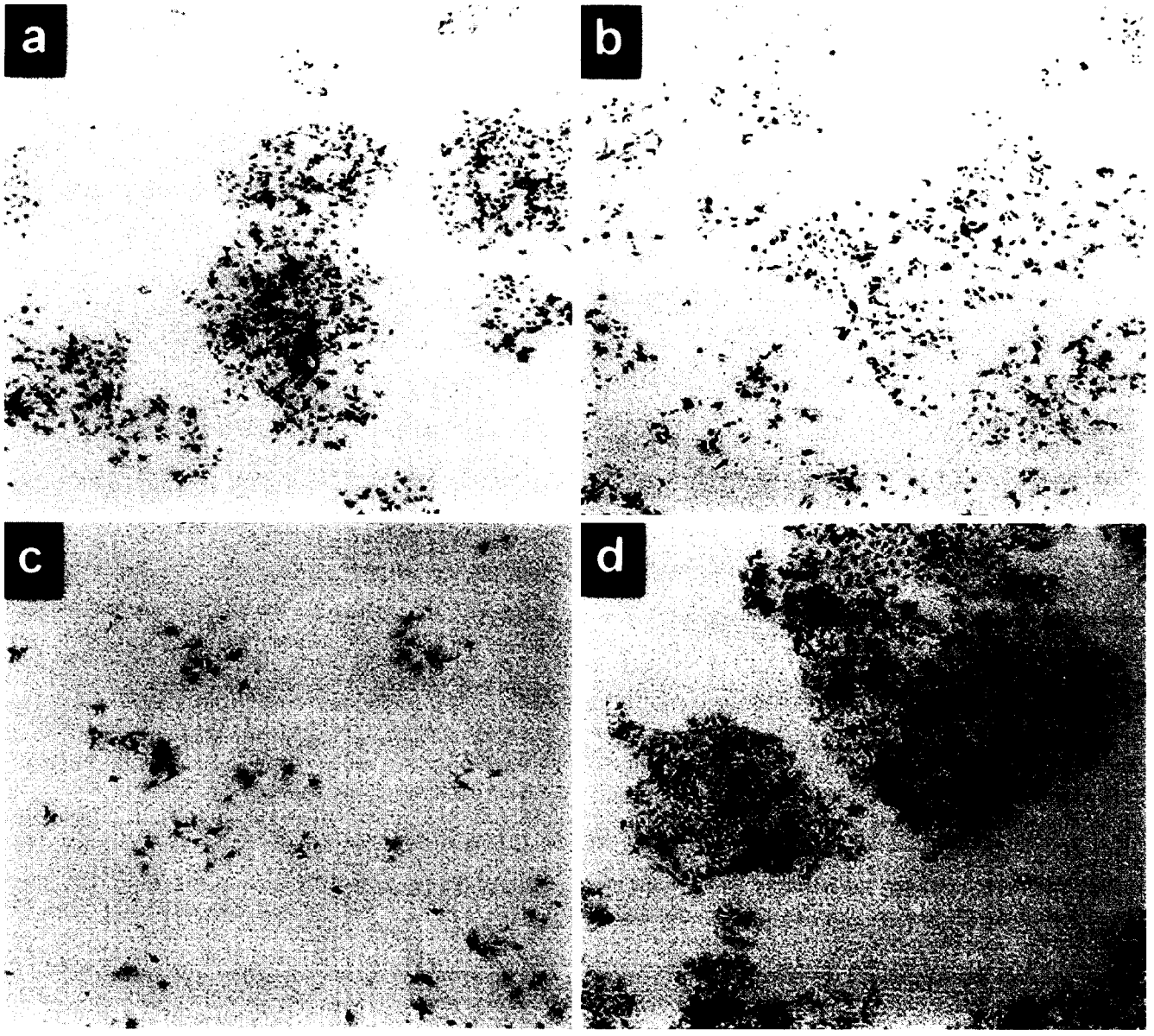

Fig. 4. p53 activation in TR3 cells at non-permissive temperature provokes a stable loss of proliferation. Hep3B-TR (a), TR4 (b) and TR3 (c, d) cells (50 000) were plated and grown at permissive temperature for 24 h. The following day (time 0) cells were either shifted to non-permissive temperature (a, b, c) or left at the permissive temperature (d), and cultivated for 7 days. Colony forming cells were then visualized by crystal violet staining. As compared to Hep3B-TR (a) and TR4 (b) cells, TR3 cells (c) did not form visible colonies at the non-permissive temperature, but maintained growth at the permissive temperature (d).

decrease in S phase cells (from 18–22% to 31–34% at different time points). In addition, the ratio of G1 cells was consistently lower at 32°C in these cells, while the ratio of G2/M cells remained essentially similar to those observed at 39°C. The apparent increase in S phase cells of TR4 at 32°C is probably due to a slow-down of DNA synthesis at low temperature. Thus, the temperature shift to 32°C had an opposite effect on TR3 cells as compared to TR4, causing a strong decrease in the fraction of S phase cells in the former. This p53-dependent effect remained effective as long as the TR3 cells were kept at 32°C (Table 1), but the fraction of S phase cells increased again when the cell culture temperature was shifted back to 39°C (data not shown).

Lack of retinoblastoma protein in Hep3B and Hep3B-TR cells

The Hep3B cell line and its TGF-β-resistant Hep3B-TR clone were tested for pRb expression. Mahlavu and

Saos-2 cells were used as positive and negative controls, respectively. Mahlavu cells express a normal-sized pRb (ref. 19), whereas Saos-2 cells express an abnormal pRb protein of 95 kDa with a C-terminal truncation due to the deletion of exons 21–27 of the retinoblastoma gene (24). Three anti-pRb monoclonal antibodies directed against distinct epitopes (IF8, Ab-5, and Ab-6) were used for Western blot and Immunoprecipitation experiments. Western immunoblotting with Ab-5 antibody (Fig. 7A) detected a single 110-kDa polypeptide in Mahlavu cell line, but not in Saos-2 and Hep3B-TR cells. The Ab-6 antibody provided a similar result, except that this antibody also reacted weakly with a smaller polypeptide in all three cell lines (Fig. 7B). With both antibodies, Hep3B-TR cells did not show any evidence of full-length pRb protein and reacted similarly to Saos-2. In a third Western blot assay using the IF8 antibody, we compared Mahlavu, Hep3B-TR and Hep3B cells. As shown in Fig. 7C, 110 kDa pRb protein was detected only in Mahlavu cell line, but not in Hep3B-TR or Hep3B cells. This antibody also reacted strongly with a smaller polypeptide in all three cell lines. However, immunoprecipitation experiments with Mahlavu and Hep3B-TR allowed detection of a single 110-kDa band in Mahlavu, but not in Hep3B-TR cells. The smaller polypeptide was not detected by this technique (Fig. 7D). Thus, it appears that, under denaturing conditions of Western blotting assays, IF8 antibody reacts with a polypeptide unrelated to pRb protein. Under the PAGE conditions used for these experiments (8% gel), pRb protein is not separated to its differentially phosphorylated forms. Therefore, it is also highly unlikely that the smaller bands observed here represent underphosphorylated forms of pRb protein.

These findings obtained with three different anti-pRb monoclonal antibodies, together with our previously published studies using a polyclonal anti-pRb

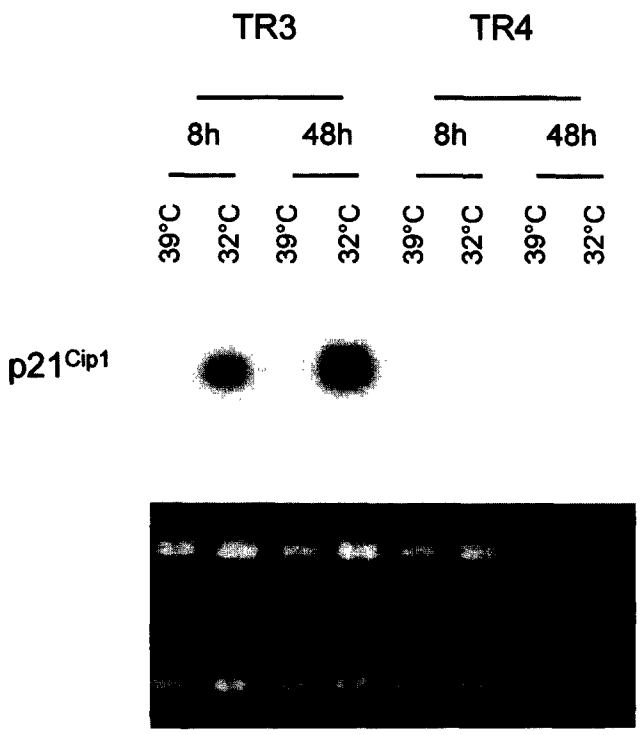

Fig. 5. p53 activation in TR3 cells at non-permissive temperature induces the expression of $p21^{Cip1}$ gene. The p53-positive TR3 and p53-negative TR4 cells were grown at either permissive (39°C) or non-permissive (32°C) temperatures for the indicated times, following overnight culture at the permissive temperature. Total RNAs were extracted and tested for $p21^{Cip1}$ transcripts by Northern blot analysis. Ethidium bromide staining of total RNAs (bottom) is also shown.

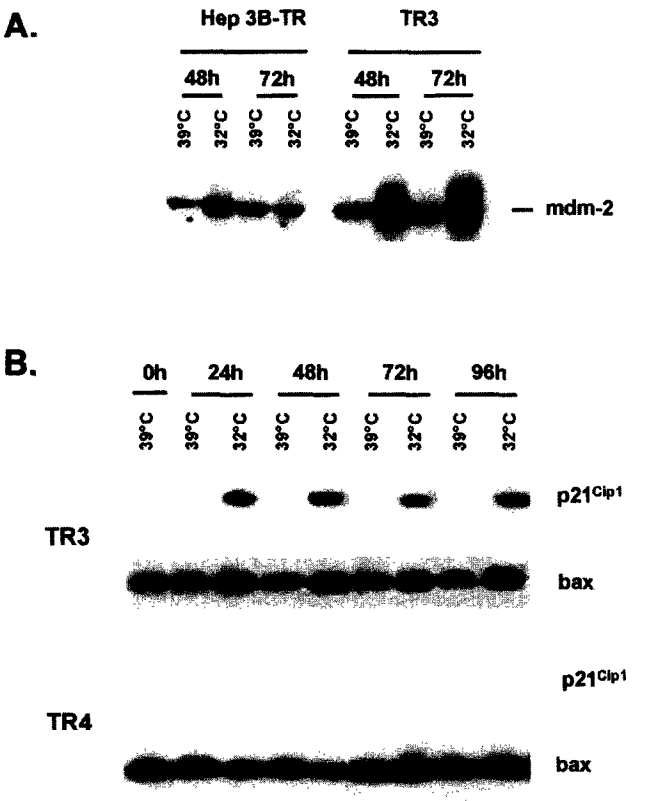

Fig. 6. p53 activation in TR3 cells at non-permissive temperature induces the accumulation of mdm-2, $p21^{Cip1}$ and bax proteins. (A) p53-positive TR3 cells were grown at permissive (39°C) or non-permissive (32°C) temperature and tested for mdm-2 protein by Western immunoblotting assay. Parental Hep3B-TR cells were used as a negative control for p53 expression. (B) p53-positive TR3 (top) and p53-negative TR4 (bottom) cells were grown as in A for the indicated times and tested for $p21^{Cip1}$ and bax proteins by Western immunoblotting assay.

TABLE 1

Effect of p53 activation on cell cycle distribution of Hep3B-TR-derived clone TR3, as compared to p53-negative control clone TR4

TR3		24 h (n=1)*	48 h (n=3)*	72 h (n=3)*
G1	32°C	52	52±6	54±7
	39°C	43	45±3	48±3
S	32°C	4	9±4	11±5
	39°C	29	23±5	20±6
G2/M	32°C	44	38±10	35±6
	39°C	29	33±3	32±3
TR4		24 h (n=1)*	48 h (n=3)	72 h (n=3)
G1	32°C	48	44±6	48±9
	39°C	53	57±1	60±2
S	32°C	32	34±3	31±6
	39°C	26	22±0	18±4
G2/M	32°C	20	21±4	22±4
	39°C	22	22±2	22±2

* n=number of experiments, % value of each fraction (mean±SD) is given.

antibody (19), clearly establish that pRb is not detectable in Hep3B and Hep3B-TR cells. Obviously, we cannot formally exclude the possibility that the pRb is present at extremely low levels in Hep3B and Hep3B-TR cells. However, it is clear that these cells are not different from Saos-2 cells in terms of normal pRb expression. Unlike us, Friedman et al. (15) were able to detect low levels of pRb protein in Hep3B cells. However, these authors reported that the pRb protein in Hep3B cells protein was not functional. Thus, despite a discrepancy for the presence of pRb, the final conclusion of both studies was that Hep3B (ref. 15 and our observations), as well as Hep3B-derived Hep3B-TR cells (our observation) were pRb-deficient. This conclusion provided a plausible explanation for the resistance of Hep3B cells to $p16^{INK4a}$ overexpression.

Accumulation of cyclin E protein in TR3 cells indicates a cell cycle arrest at the G1/S transition

The G1 growth arrest induced by p53 in TR3 cells was accompanied by an accumulation of $p21^{Cip1}$ protein due to a p53-dependent increase in $p21^{Cip1}$ gene expression. This protein acts as an inhibitor of CDK2/cyclin E complexes during the late stage of the G1 phase (17). To test any effect of $p21^{Cip1}$ accumulation on cyclin E and CDK2 protein levels, we analyzed these two proteins by Western immunoblotting at time zero, 8 h, 24 h, 48 h and 72 h in TR3 and TR4 cells grown at either 32°C or 39°C. As shown in Fig. 8, basal levels of CDK2 protein were high in TR3 cells, and they remained constant for at least 72 h, independent of growth temperature. Cyclin E protein was weakly detectable at time zero. At non-permissive temperature (32°C), there was no change at 8 h, but a strong and continued increase was observed at times 24 h, 48 h and 72 h. At permissive temperature (39°C), there was also a slight and continued accumulation of cyclin E in these cells. This was probably due to a slow increase in the number of cells at G1 phase as a result of increased confluency of cells. However, even at 72 h, these levels remained far below the levels observed at the non-permissive tempeature (Fig. 8). Studies with the negative control cell line TR4 were also shown in Fig. 8, for comparison. Basal levels of CDK2 were also high in this clone at early times (first 24 h), but slightly lower CDK2 levels were detected thereafter. Cyclin E

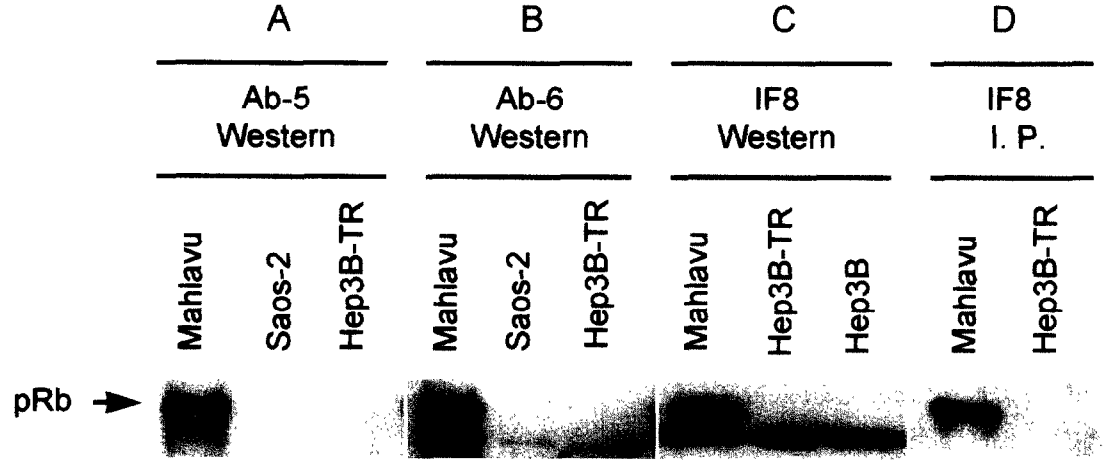

Fig. 7. The absence of detectable retinoblastoma protein (pRb) in Hep3B and Hep3B-TR cells. Lysates were tested for pRb protein by either Western blotting (A, B, C) or immunoprecipitation from [^{35}S]-methionine-labeled cells (D). pRb protein was tested with monoclonal antibodies Ab-5 (A), Ab-6 (B) and IF8 (C, D). Mahlavu and Saos-2 cells were used as positive and negative controls, respectively.

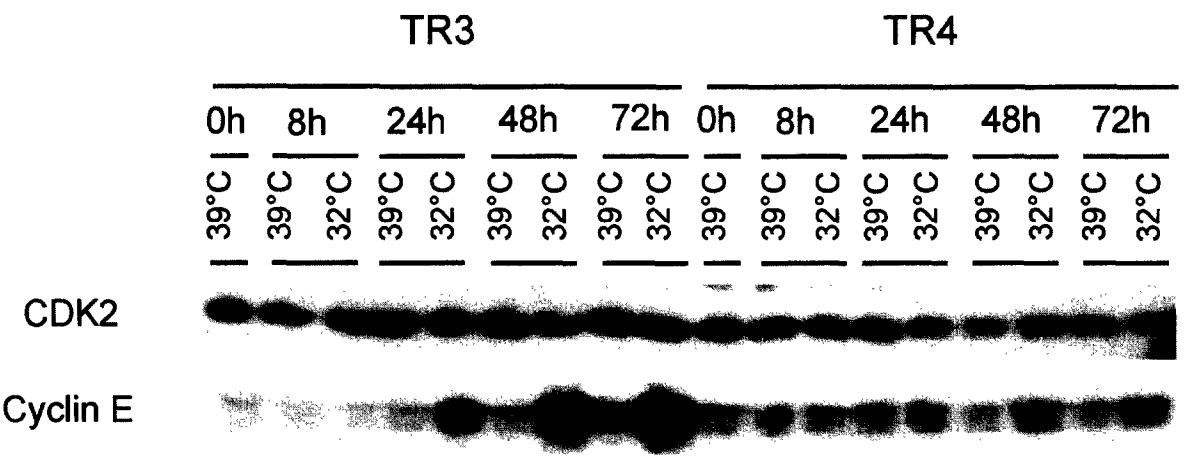

Fig. 8. Accumulation of cyclin E protein in TR3 cells following p53 activation. TR3 and TR4 clones were grown at either non-permissive (32°C) or permissive (39°C) temperature for the indicated times and cell lysates were tested for cyclin-dependent kinase 2 (CDK2) and cyclin E protein levels by Western immunoblotting.

levels, low at time zero remained essentially the same at 39°C, but there was a slight increase at 32°C. Strong accumulation of cyclin E in TR3 cells at non-permissive temperature was a consequence of p53 activation, but the delayed accumulation suggested that this change was not due to the direct transactivation of cyclin E gene by p53. As reported in Fig. 5, the response of p21^{Cip1}, a direct target of p53 was detectable as early as 8 h, whereas cyclin E accumulation started at 24 h.

Discussion

We compared the effects of p53 and p16^{INK4a} proteins in pRb protein-deficient hepatocellular carcinoma cells. The overexpression of p16^{INK4a} did not affect the cell growth rate. To our knowledge, the effects of p16^{INK4a} in hepatoma cells have not been reported previously. Spillare et al. (25) reported that the number of colonies of Hep3B cells following a transfection with a p16^{INK4a} expression plasmid was about 30% lower than those obtained with a control plasmid and 50% of colonies expressed the transfected p16^{INK4a} cDNA. Thus, both the weak effect of p16^{INK4a} transfection on colony formation and the *in vitro* growth of at least 50% of colonies despite p16^{INK4a} overexpression also confirm our hypothesis that Hep3B cells can tolerate p16^{INK4a} overexpression. Moreover, studies with other cell types demonstrated that pRb-deficient cell lines are resistant to G1 phase growth arrest by p16^{INK4a} protein (26–29). As illustrated in Fig. 9, p16^{INK4a} indirectly blocks cell cycle progression by inhibiting the release of "free E2F" transcription factors from the pRb/E2F complexes by CDK4-catalyzed phosphorylation of pRb protein (30). In cells lacking pRb protein, the availability of "free E2F" transcription factors (more specifically E2F-1, E2F-2 and E2F-3) is no longer controlled.

In contrast to p16^{INK4a}, the overexpression of wild-type p53 in pRb-deficient hepatoma cells provoked a strong and sustained growth inhibition. This effect was consistent with our previous studies showing that *in vitro* growth of these cells was not compatible with the expression of wild-type p53, in contrast to p53-249Ser mutant (11,22). Other studies with Hep3B cell line reported that wild-type p53 induce apoptotic cell death

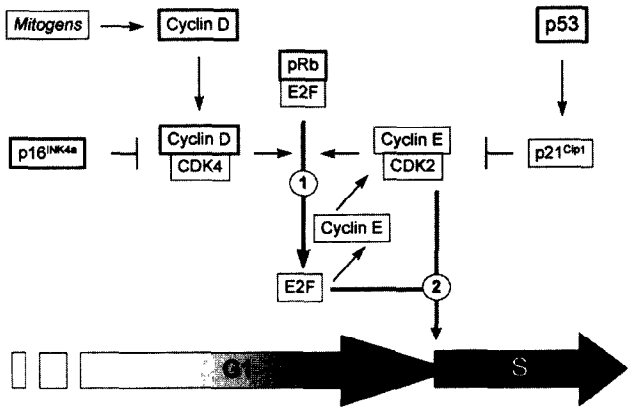

Fig. 9. A model highlighting the roles of cyclin D, p16^{INKa}, pRb and p53 gene mutations in the loss of cell cycle control in human hepatocellular carcinoma. The numbers 1 and 2 indicate the two critical steps of cell cycle progression at the G1 phase. The step 1 is controlled mainly by cyclin D/CDK4 activity on pRb phosphorylation and E2F release. The step 2 is controlled by both E2F and cyclin-E/CDK2 activity for the transition from G1 to S phase. In pRb-negative cells, step 1 is not inhibited by p16^{INK4a}, but step 2 is inhibited by p53 via p21^{Cip}.

(12–14), with the exception of one study reporting that these cells were resistant to p53-induced apoptosis and growth arrest (15). Both the choice of cell line (TGF-β-resistant Hep3B-TR clone in our studies in contrast to TGF-β-sensitive parental Hep3B cells used in others) and different experimental conditions could effect the outcome of experiments. The use of a mouse mutant p53-135val expression vector in this study contrast with the use of human wild-type p53 in previously reported apoptosis studies (12–14). Although the mouse mutant p53 used here was initially used to demonstrate p53-mediated apoptosis (31), we cannot exclude the possibility that this particular protein is unable to induce apoptosis in Hep3B-TR cells.

The p53-mediated growth arrest in Hep3B-TR clones was confirmed by three independent tests including thymidine incorporation, flow cytometry and *in vitro* long-term growth assays. The mechanism by which p53 induces growth arrest in Hep3B-TR cells is not known yet, but our observations are in favor of the following hypothesis: p53 activation in these cells causes an accumulation of $p21^{Cip1}$ protein leading to an inhibition of kinase activity of CDK2/cyclin E complexes. Recent studies, as reviewed by Sherr & Roberts (17), showed that G1 phase cell cycle inhibition by $p21^{Cip1}$ (as well as other members of Cip/Kip family of proteins) is concordant with specific inhibition of cyclin E-dependent CDK2 rather than cyclin D-dependent CDK4 enzyme (Fig. 9). The active CDK2/cyclin E complexes have at least two different functions in cell cycle progression: (1) further phosphorylation of pRb allowing an amplification of "free E2F" release from pRb/E2F complexes; (2) phosphorylation of other proteins (i.e. NPAT) involved in G1/S transition (17,30,32). It is expected that, in pRb-negative cells, the first function is no longer needed and the second function becomes rate-limiting. Indeed, cyclin E is able to induce S phase entry without activation of the retinoblastoma/E2F pathway (33), suggesting that CDK2/cyclin E-mediated S phase entry is independent of pRb protein. In Hep3B-TR cells, p53-induced growth arrest was accompanied by a progressive accumulation of cyclin E, as well as $p21^{Cip1}$ protein. Cyclin E gene is known to be activated by E2F factors (30). Thus, the accumulation of cyclin E may be taken as evidence that, in these pRb-negative cells, pRb-dependent E2F molecules (E2F-1, E2F-2 or E2F-3) are "free" (30). However, this accumulation of cyclin E lasted at least 72 h (Fig. 8) and was accompanied by a loss of DNA synthesis (Fig. 3), rather than entry into S phase. This pattern differs from the fluctuating pattern of cyclin E protein levels (and CDK2/cyclin E activity) in proliferating cells with peak levels at G1/S transition followed by a loss at early S phase (34). We did not test CDK2/cyclin E enzyme activity in our cells, but the pattern of cyclin E accumulation and DNA synthesis inhibition suggest that, following p53 activation, cells are able to progress in the early G1 phase of cell cycle (no functional pRb), but are maintained at the G1/S transition because of $p21^{Cip1}$-mediated inhibition of CDK2/cyclin E enzyme activity. Alternatively, cyclin E accumulation could be linked to a direct induction of cyclin E gene expression by p53, but cyclin E gene is not a known target of p53. As a first conclusion, our observations clearly indicate that the p53 is able to provoke a G1 arrest independent of "retinoblastoma pathway" in hepatoma cells and that this "retinoblastoma-independent pathway" may involve the inhibition of phosphorylation of no-pRb proteins such as NPAT by CDK2/cyclin E complexes.

With regard to genetic changes observed in HCC, it appears that, in one group of tumors, genetic changes affecting retinoblastoma, cyclin D and $p16^{INK4a}$ genes lead to a loss of growth control in early G1 phase of cell proliferation. As demonstrated here with a pRb-deficient cell line, in this group of tumors, p53-mediated growth control leading to a late G1 phase arrest remains functional. Another group of tumors displays alterations in p53 gene. In these tumors, a functional retinoblastoma pathway may still protect cells against a severe loss of growth control. The worst situation would be with a third group of tumors displaying alterations in both p53 and retinoblastoma pathway genes with almost a total loss of growth control of G1 phase (Fig. 9). HCCs displaying alterations on both p53 and retinoblastoma genes have been described (35). This peculiar situation could explain why the prognostic value of individual genetic changes in HCC was not rewarding. A systematic study of several gene alterations in these tumors might provide better information for disease prognosis.

Acknowledgements

We thank A. Fattaey, M. Oren, J. Samarut, T. Soussi and B. Vasylyk for providing some of the reagents used here. This work was supported by grants to M. O. from INSERM, TÜBITAK and TWAS. K. U. was a recipient of a BDP fellowsip from TÜBITAK.

References

1. Strauss RM. Hepatocellular carcinoma: clinical, diagnostic, and therapeutic aspects. In: Rustgi AK, editor. Gastrointestinal Cancers: Biology, Diagnosis and Therapy. Philadelphia: Lippincott-Raven Publishers; 1995. p. 479–96.
2. Ozturk M. Genetic aspects of hepatocellular carcinogenesis. Semin Liver Dis 1999; 19: 235 42.
3. Bressac B, Galvin KM, Liang TJ, Isselbacher KJ, Wands JR,

Ozturk M. Abnormal structure and expression of p53 gene in human hepatocellular carcinoma. Proc Natl Acad Sci USA 1990; 87: 1973–7.
4. Bressac B, Kew M, Wands J, Ozturk M. Selective G to T mutations of p53 gene in hepatocellular carcinoma from southern Africa. Nature 1991; 350: 429–31.
5. Hsu IC, Metcalf RA, Sun T, Welsh JA, Wang NJ, Harris CC. Mutational hotspot in the p53 gene in human hepatocellular carcinomas. Nature 1991; 350: 427–8.
6. Wang XW, Forrester K, Yeh H, Feitelson MA, Gu JR, Harris CC. Hepatitis B virus X protein inhibits p53 sequence-specific DNA binding, transcriptional activity, and association with transcription factor ERCC3. Proc Natl Acad Sci USA 1994; 91: 2230–4.
7. Ueda H, Ullrich SJ, Gangemi JD, Kappel CA, Ngo L, Feitelson MA, et al. Functional inactivation but not structural mutation of p53 causes liver cancer. Nat Genet 1995; 9: 41–7.
8. Elmore LW, Hancock AR, Chang SF, Wang XW, Chang S, Callahan CP, et al. Hepatitis B virus X protein and p53 tumor suppressor interactions in the modulation of apoptosis. Proc Natl Acad Sci USA 1997; 94: 14707–12.
9. Levine AJ. p53, the cellular gatekeeper for growth and division. Cell 1997; 88: 323–31.
10. Prives C. Signalling to p53: breaking the MDM2-p53 circuit. Cell 1998; 95: 5–8.
11. Puisieux A, Ponchel F, Ozturk M. p53 as a growth suppressor gene in HBV-related hepatocellular carcinoma cells. Oncogene 1993; 8: 487–90.
12. Zhuang SM, Shvarts A, Jochemsen AG, van Oorschot AA, van der Eb AJ, Noteborn MH. Differential sensitivity to Ad5 E1B-21kD and Bcl-2 proteins of apoptin-induced versus p53-induced apoptosis. Carcinogenesis 1995; 16: 2939–44.
13. Roemer K, Mueller-Lantzsch N. p53 transactivation domain mutant Q22, S23 is impaired for repression of promoters and mediation of apoptosis. Oncogene 1996; 12: 2069–79.
14. Mitry RR, Sarraf CE, Wu CG, Pignatelli M, Habib NA. Wild-type p53 induces apoptosis in Hep3B through up-regulation of bax expression. Lab Invest 1997; 77: 369–78.
15. Friedman SL, Shaulian E, Littlewood T, Resnitzky D, Oren M. Resistance to p53-mediated growth arrest and apoptosis in Hep3B hepatoma cells. Oncogene 1997; 15: 63–70.
16. Chin L, Pomerantz J, DePinho RA. The INK4a/ARF tumor suppressor: one gene – two products – two pathways. Trends Biochem Sci 1998; 23: 291–6.
17. Sherr CJ, Roberts JM. CDK inhibitors: positive and negative regulators of G1-phase progression. Genes Dev 1999; 13: 1501–12.
18. Inagaki M, Moustakas A, Lin HY, Lodish HF, Carr BI. Growth inhibition by transforming growth factor beta (TGF-beta) type I is restored in TGF-beta-resistant hepatoma cells after expression of TGF-beta receptor type II cDNA. Proc Natl Acad Sci USA 1997; 90: 5359–63.
19. Puisieux A, Galvin K, Troalen F, Bressac B, Marcais C, Galun E, et al. Retinoblastoma and p53 tumor suppressor genes in human hepatoma cell lines. FASEB J 1993; 7: 1407–13.
20. Michalovitz D, Halevy O, Oren M. Conditional inhibition of transformation and of cell proliferation by a temperature-sensitive mutant of p53. Cell 1990; 62: 671–80.
21. Rouault J-P, Falette N, Guehenneux F, Guillot C, Rimokh R, Wang Q, et al. Identification of BTG2, an antiproliferative p53-dependent component of the DNA damage cellular response pathway. Nat Genet 1996; 14: 482–6.
22. Ponchel F, Puisieux A, Tabone E, Michot J-P, Froschl G, Morel A-P, et al. Hepatocarcinoma-specific mutant p53-249ser induces mitotic activity but has no effect on transforming growth factor beta 1-mediated apoptosis. Cancer Res 1994; 54: 2064–8.
23. Legros Y, Meyer A, Ory K, Soussi T. Mutations in p53 produce a common conformational effect that can be detected with a panel of monoclonal antibodies directed toward the central part of the p53 protein. Oncogene 1994; 9: 3689–94.
24. Shew JY, Lin BT, Chen PL, Tseng BY, Yang-Feng TL, Lee WH. C-terminal truncation of the retinoblastoma gene product leads to functional inactivation. Proc Natl Acad Sci USA 1990; 87: 6–10.
25. Spillare EA, Okamoto A, Hagiwara K, Demetric DJ, Serrano M, Deach D, et al. Suppression of growth *in vitro* and tumorigenicity *in vivo* of human carcinoma cells by transfected p16^{INK4a}. Mol Carcinogen 1996; 16: 53–60.
26. Guan K-L, Jenkins CW, Li Y, Nichols MA, Wu X, O'Keefe CL, et al. Growth suppression by p18, a p16INK4/MTS1- and p15INK4b/MTS2-related CDK6 inhibitor, correlates with wild-type pRb function. Genes Dev 1994; 8: 2939–52.
27. Koh J, Enders GH, Dyntacht BD, Harlow E. Tumour-derived p16 alleles encoding proteins defective in cell-cycle inhibition. Nature 1995; 375: 506–10.
28. Lukas J, Parry D, Aagaard L, Mann DJ, Bartkova J, Strauss M, et al. Retinoblastoma protein-dependent cell cycle inhibition by the tumor suppressor p16. Nature 1995; 375: 503–6.
29. Medema RH, Herrera RE, Lam F, Weinberg RA. Growth suppression by p16ink4 requires functional retinoblastoma protein. Proc Natl Acad Sci USA 1995; 92: 6289–93.
30. Dyson N. The regulation of E2F by pRB-family proteins. Genes Dev 1998; 12: 2245–62.
31. Yonish-Rouach E, Resnitzky D, Lotem J, Sachs L, Kimchi A, Oren M. Wild-type p53 induces apoptosis of myeloid leukaemic cells that is inhibited by interleukin-6. Nature 1991; 352: 345–7.
32. Zhao J, Dynlacht B, Imai T, Hori T, Harlow E. Expression of NPAT, a novel substrate of cyclin E-CDK2, promotes S-phase entry. Genes Dev 1998; 12: 456–61.
33. Lukas J, Herzinger T, Hansen K, Moroni MC, Resnitzky D, Helin K, et al. Cyclin E-induced S phase without activation of the pRb/E2F pathway. Genes Dev 1997; 11: 1479–92.
34. Dulic V, Lees E, Reed SI. Association of human cyclin E with a periodic G1-S phase protein kinase. Science 1992; 257: 1958–61.
35. Murakami Y, Hayashi K, Hirohashi S, Sekiya T. Aberrations of the tumor suppressor p53 and retinoblastoma genes in human hepatocellular carcinomas. Cancer Res 1991; 51: 5520–5.